Quantum Geometry and Nonlinear Electromagnetic Responses of Solids

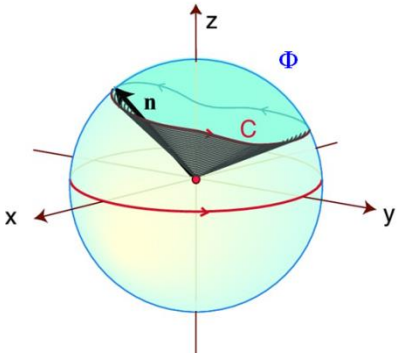

Guang-Yu Guo (郭光宇)

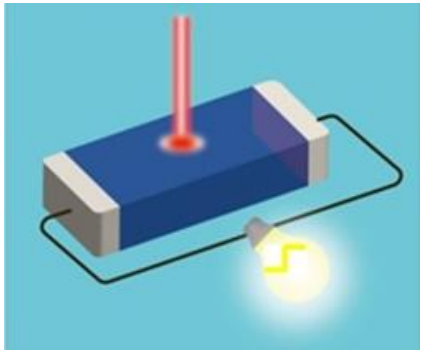

Physics Division, National Center for Theoretical Sciences

Department of Physics, National Taiwan University

(Talk in NCTS-iTHEMS (RIKEN) Joint Workshop,
National Center for Theoretical Center, Taipei, Aug. 26-29, 2024)

Plan of this Talk

I. Introduction to quantum geometry

II. Responses of solids to static electromagnetic fields

III. Nonlinear optical responses of solids

IV. Summary

I. Introduction to quantum geometry

1. Concept of quantum geometry

(Classical) geometry studies the properties of objects in real space

e.g., distance, area
and curvature etc.

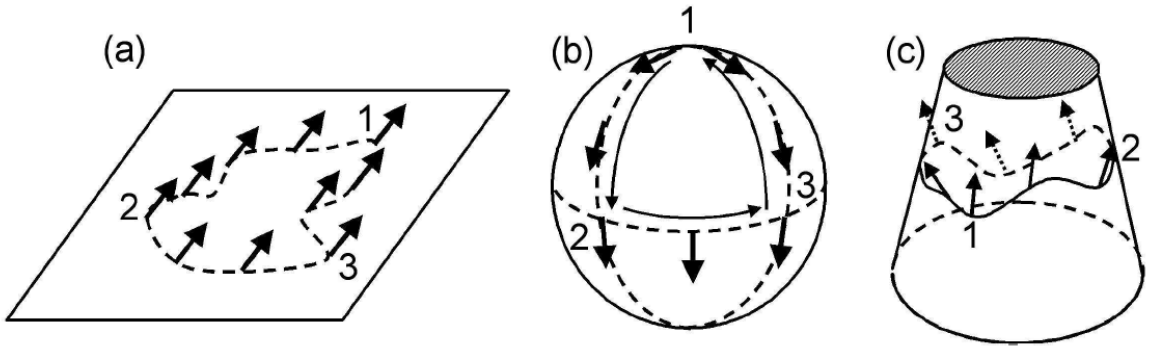

Figure from [Bruno, cond-mat/0506270 (2005)]

Quantum geometry

In quantum physics, eigenvalues and eigenstates of the Schrödinger equation fully describe the physical behavior of a system. Let us assume Hamiltonian has a parametric dependence and the Schrödinger equation is

$$\hat{H}(\boldsymbol{\kappa})\psi_{n\boldsymbol{\kappa}}(\mathbf{r}) = \varepsilon_{n\boldsymbol{\kappa}}\psi_{n\boldsymbol{\kappa}}(\mathbf{r})$$

where $\boldsymbol{\kappa}$ is the d-dimensional real parameter.

Quantum geometry studies the geometric structure of the eigenstate space.

Quantum distance, metric tensor and gauge invariance

Upon a small variation of parameter $d\boldsymbol{\kappa}$, the distance between two neighboring quantum states

$$ds^2 = \left\| \psi_{n(\boldsymbol{\kappa}+d\boldsymbol{\kappa})} - \psi_{n\boldsymbol{\kappa}} \right\|^2 = \left\langle \delta\psi_{n\boldsymbol{\kappa}} \,|\, \delta\psi_{n\boldsymbol{\kappa}} \right\rangle$$
$$= \left\langle \partial_a \psi_{n\boldsymbol{\kappa}} \,|\, \partial_a \psi_{n\boldsymbol{\kappa}} \right\rangle d\kappa^a d\kappa^b = (\gamma^n_{ab}(\boldsymbol{\kappa}) + i\sigma^n_{ab}(\boldsymbol{\kappa}))d\kappa^a d\kappa^b .$$

[Provost & Vallee, Commun Math Phys 76 (1980) 289]
[Ma et al., PRB 81 (2010) 245129]
[Resta, Eur Phys J B 79 (2011) 121]
[Cheng, arXiv:1012.1337 (2013)]

Since $\left\langle \partial_a \psi_{n\boldsymbol{\kappa}} \,|\, \partial_a \psi_{n\boldsymbol{\kappa}} \right\rangle$ is Hermitian, $\gamma^n_{ab} = \gamma^n_{ba}$, $\sigma^n_{ab} = -\sigma^n_{ba}$, $\sigma^n_{ab} d\kappa^a d\kappa^b = 0$.

[Note: $\partial_a = \partial_{\kappa_a}$]

Thus, $ds^2 = \gamma^n_{ab} d\kappa^a d\kappa^b$ and γ^n_{ab} looks like the metric tensor.

However, γ_{ab} is not gauge invariant. Instead, one can define the gauge invariant metric

$$g^n_{ab}(\boldsymbol{\kappa}) := \gamma^n_{ab}(\boldsymbol{\kappa}) - A^n_a(\boldsymbol{\kappa}) A^n_b(\boldsymbol{\kappa})$$

where $A^n_a(\boldsymbol{\kappa}) = i\left\langle \psi_{n\kappa}(\boldsymbol{\kappa}) \middle| \partial_a \psi_{n\kappa}(\boldsymbol{\kappa}) \right\rangle$ is the Berry connection.

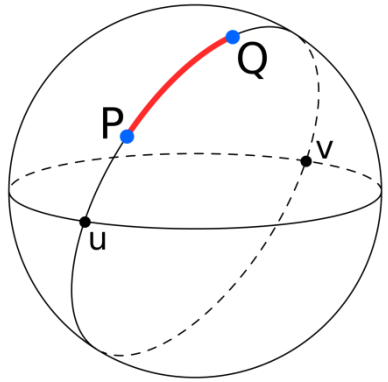

Thus, g_{ab} ($\boldsymbol{\kappa}$) measures the distance between two quantum states in Projected Hilbert space $PH = H/U(1)$ while measures the distance of "bare states" in Hilbert space H.

The "geodesic quantum distance" between two quantum states $\boldsymbol{\kappa}_P$ and $\boldsymbol{\kappa}_Q$ is given by

$$\left\langle \psi_{n\boldsymbol{\kappa}_Q} \middle| \psi_{n\boldsymbol{\kappa}_P} \right\rangle = 1 - \frac{1}{2} \int_{\boldsymbol{\kappa}_P}^{\boldsymbol{\kappa}_Q} g^n_{ab}(\boldsymbol{\kappa}) d\kappa^a d\kappa^b .$$

Berry curvature and quantum geometric tensor (Hermitian metric)

One can define the gauge invariant "quantum geometric tensor" (QGT) as

$$\mathrm{Q}^n_{ab}(\boldsymbol{\kappa}) := \langle \partial_a \psi_{n\boldsymbol{\kappa}} \,|\, \partial_b \psi_{n\boldsymbol{\kappa}} \rangle - \langle \partial_a \psi_{n\boldsymbol{\kappa}} \,|\, \psi_{n\boldsymbol{\kappa}} \rangle \langle \psi_{n\boldsymbol{\kappa}} \,|\, \partial_b \psi_{n\boldsymbol{\kappa}} \rangle = g^n_{ab}(\boldsymbol{\kappa}) + i\sigma^n_{ab}(\boldsymbol{\kappa})$$

with $g^n_{ab}(\boldsymbol{\kappa}) = \mathrm{Re}\, Q^n_{ab}(\boldsymbol{\kappa})$ and $\sigma^n_{ab}(\boldsymbol{\kappa}) = \mathrm{Im}\, Q^n_{ab}(\boldsymbol{\kappa})$.

Since $\langle \partial_a \psi_{n\boldsymbol{\kappa}} \,|\, \psi_{n\boldsymbol{\kappa}} \rangle \langle \psi_{n\boldsymbol{\kappa}} \,|\, \partial_b \psi_{n\boldsymbol{\kappa}} \rangle$ is real, [Xiao, Chang & Niu, RMP 82 (2010) 1959]

$$\sigma^n_{ab}(\boldsymbol{\kappa}) = \mathrm{Im}\, Q^n_{ab}(\boldsymbol{\kappa}) = \mathrm{Im} \langle \partial_a \psi_{n\boldsymbol{\kappa}} \,|\, \partial_b \psi_{n\boldsymbol{\kappa}} \rangle = -\frac{i}{2}\left[\langle \partial_a \psi_{n\boldsymbol{\kappa}} \,|\, \partial_b \psi_{n\boldsymbol{\kappa}} \rangle - \langle \partial_b \psi_{n\boldsymbol{\kappa}} \,|\, \partial_a \psi_{n\boldsymbol{\kappa}} \rangle \right]$$

$$= -\frac{1}{2}\left[\partial_a A^n_b(\boldsymbol{\kappa}) - \partial_b A^n_a(\boldsymbol{\kappa}) \right] = -\frac{1}{2}\Omega^n_{ab}(\boldsymbol{\kappa}) \,.$$

Berry phase

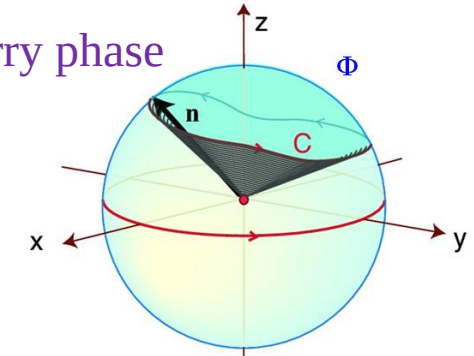

$$\Phi = \oint_C \mathbf{A} \cdot d\mathbf{l} = \int_S \boldsymbol{\Omega} \cdot d\mathbf{S}$$

$$\boldsymbol{\Omega} = \nabla \times \mathbf{A}$$

Thus, $Q^n_{ab}(\boldsymbol{\kappa}) = g^n_{ab}(\boldsymbol{\kappa}) - \frac{i}{2}\Omega^n_{ab}(\boldsymbol{\kappa})$,

where $\Omega^n_{ab}(\boldsymbol{\kappa})$ is the Berry Curvature.

QGT can be rewritten as [Resta, Eur Phys J B 79 (2011) 121]

$$\mathrm{Q}^n_{ab}(\boldsymbol{\kappa}) = \sum_{m \neq n} \frac{\langle \psi_{n\boldsymbol{\kappa}} \,|\, \partial_a H(\boldsymbol{\kappa}) \,|\, \psi_{m\boldsymbol{\kappa}} \rangle \langle \psi_{m\boldsymbol{\kappa}} \,|\, \partial_b H(\boldsymbol{\kappa}) \,|\, \psi_{n\boldsymbol{\kappa}} \rangle}{\left[\varepsilon_n(\boldsymbol{\kappa}) - \varepsilon_m(\boldsymbol{\kappa}) \right]^2}.$$

Thus, $\Omega^n_{ab}(\boldsymbol{\kappa}) = -2\,\mathrm{Im}\left[\sum_{m \neq n} \frac{\langle \psi_{n\boldsymbol{\kappa}} \,|\, \partial_a H(\boldsymbol{\kappa}) \,|\, \psi_{m\boldsymbol{\kappa}} \rangle \langle \psi_{m\boldsymbol{\kappa}} \,|\, \partial_b H(\boldsymbol{\kappa}) \,|\, \psi_{n\boldsymbol{\kappa}} \rangle}{\left[\varepsilon_n(\boldsymbol{\kappa}) - \varepsilon_m(\boldsymbol{\kappa}) \right]^2} \right]$.

[Carollo et al., PhysRep 838 (2020) 1]

2. Electronic band theory of solids

Band theory of electrons in solids developed by Bloch in 1928, is one of most successful theories in condensed matter physics.

It provides a simple way to classify solids into insulators, metals, semiconductors and semimetals.

It allows us to evaluate the dynamical properties of electrons in a solid needed in the semiclassical transport theory, e.g., momentum, group velocity and mass.

Before 1980's, studies in condensed matter physics focused almost exclusively on the geometry of eigenvalues (Bloch energy bands) of the Schrödinger equation.

Band geometry

(structure of eigenvalues)

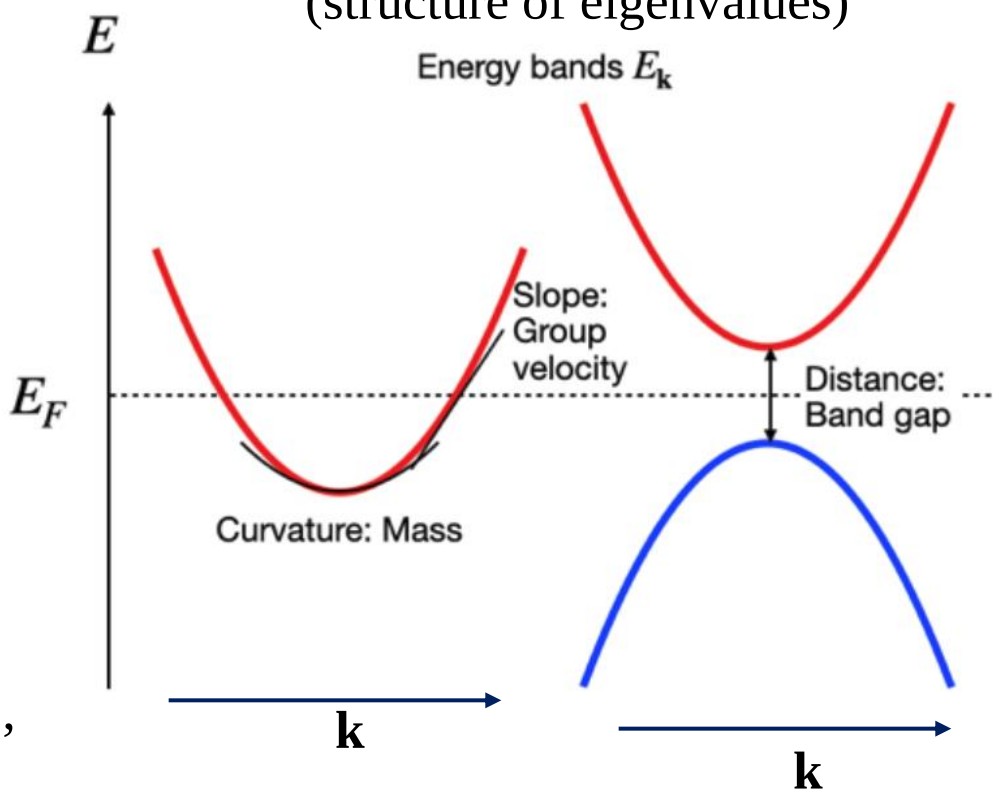

Group velocity $\mathbf{v}(\mathbf{k}) = \frac{1}{\hbar}\nabla_{\mathbf{k}} E(\mathbf{k})$

Effective mass $[\mathrm{M}^{-1}(\mathbf{k})]_{ab} = \pm\frac{1}{\hbar^2}\frac{\partial^2 E(\mathbf{k})}{\partial k_a \partial k_b}$.

3. Quantum geometry in solid state physics

Quantum geometry studies the geometric structure of Bloch functions in a band. It focus on the bands which may have nontrivial geometric quantities.

[Törmä, PRL 131 (2023) 240001]

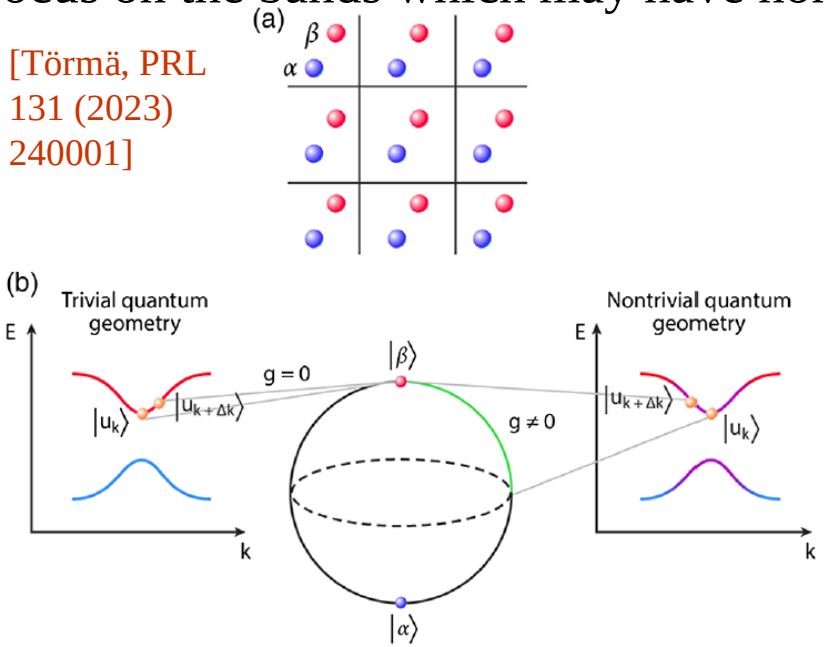

(a) Atoms in a solid form a lattice with each unit cell having 2 orbitals α and β. The $|\alpha\rangle$ and $|\beta\rangle$ states are orthogonal and the geometry of the eigenstate space is the same as that of Bloch sphere (b), which illustrates how two sets of identical band dispersions can have very different quantum metric, i.e., $g = 0$ (left) and $g \neq 0$ (right).

In recent years, it has been predicted that quantum geometry governs a variety of phenomena in solids. Studies of quantum geometry help to better understand nature, solve outstanding puzzels and also lead to new discoveries (e.g., see PRL 131 (2023) 240001 and also some talks in this workshop).

In the rest of this talk, I will present several examples of my own interest to illustrate how the quantum geometry may dominate the responses of a solid to both static and optical electromagnetic fields.

II. Responses of solids to static electromagnetic fields

1. Linear Hall effects due to Berry curvature

Electron dynamics in electromagnetic fields

Classic version [e.g., Book by Aschroft & Mermin, 1976]

$$\dot{\mathbf{r}} = \frac{1}{\hbar}\frac{\partial \varepsilon_n(\mathbf{k})}{\partial \mathbf{k}},\ \dot{\mathbf{k}} = -\frac{e}{\hbar}\mathbf{E} - \frac{e}{\hbar}\dot{\mathbf{r}}\times\mathbf{B} = \frac{e}{\hbar}\frac{\partial V(\mathbf{r})}{\partial \mathbf{r}} - \frac{e}{\hbar}\dot{\mathbf{r}}\times\mathbf{B}.$$

Berry phase correction [Chang & Niu, PRL 75, 1348 (1995); Xiao, Chang & Niu, RMP 82, 1959 (2010)]

$$\dot{\mathbf{r}} = \frac{1}{\hbar}\frac{\partial \varepsilon_n(\mathbf{k})}{\partial \mathbf{k}} + \dot{\mathbf{k}}\times\boldsymbol{\Omega}_n(\mathbf{k}),\ \dot{\mathbf{k}} = \frac{e}{\hbar}\frac{\partial V(\mathbf{r})}{\partial \mathbf{r}} - \frac{e}{\hbar}\dot{\mathbf{r}}\times\mathbf{B},$$

$$\boldsymbol{\Omega}_n(\mathbf{k}) = -\,\mathrm{Im}\left\langle \frac{\partial u_{n\mathbf{k}}}{\partial \mathbf{k}} \right| \times \left| \frac{\partial u_{n\mathbf{k}}}{\partial \mathbf{k}} \right\rangle. \quad \text{(Berry curvature)}$$

Symmetry of Berry curvature

Under *T*-symmetry: $\Omega_n(-\mathbf{k}) = -\Omega_n(\mathbf{k})$

Under *P*-symmetry: $\Omega_n(-\mathbf{k}) = \Omega_n(\mathbf{k})$

Both *T* & *P*-symmetry: $\Omega_n(\mathbf{k}) = 0$

[Xiao, Yao & Niu, PRL 99, 236809 (2007)]

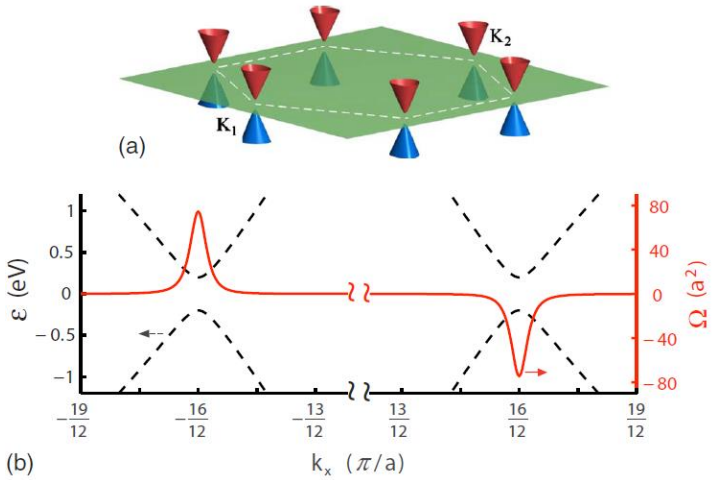

(a) Energy bands and (b) Berry curvature of a graphene sheet with broken *P*-Symmetry.

Anomalous Hall effect

Semiclassical transport theory

$$\mathbf{j} = \int d^3k(-e\dot{\mathbf{r}})g(\mathbf{r},\mathbf{k}),\quad g(\mathbf{r},\mathbf{k}) = f(\mathbf{k}) + \delta f(\mathbf{r},\mathbf{k})$$

$$\dot{\mathbf{r}} = \frac{\partial \varepsilon_n(\mathbf{k})}{\hbar \partial \mathbf{k}} + \dot{\mathbf{k}} \times \boldsymbol{\Omega} = \frac{\partial \varepsilon_n(\mathbf{k})}{\hbar \partial \mathbf{k}} - \frac{e}{\hbar}\mathbf{E} \times \boldsymbol{\Omega}$$

$$\mathbf{j} = -\frac{e^2}{\hbar}\mathbf{E} \times \int d^3\mathbf{k} f(\mathbf{k})\boldsymbol{\Omega} - \frac{e}{\hbar}\int d^3\mathbf{k}\delta f(\mathbf{k},\mathbf{r})\frac{\partial \varepsilon_n(\mathbf{k})}{\partial \mathbf{k}}$$

(Anomalous Hall conductance) (ordinary conductance)

Anomalous Hall conductivity [Yao, et al., PRL 92(2004) 037204]

$$\sigma_{yx} = J_y / E_x = -\frac{e^2}{\hbar}\int d^3k \sum_n f(\varepsilon_n(\mathbf{k}))\Omega_n^z(\mathbf{k})$$

$$\Omega_n^z(\mathbf{k}) = -\sum_{m \neq n} \frac{2\,\mathrm{Im}\langle n\mathbf{k}|v_y|m\mathbf{k}\rangle\langle m\mathbf{k}|v_x|n\mathbf{k}\rangle}{(\omega_{\mathbf{k}m} - \omega_{\mathbf{k}n})^2}$$

Anomalous Hall effect

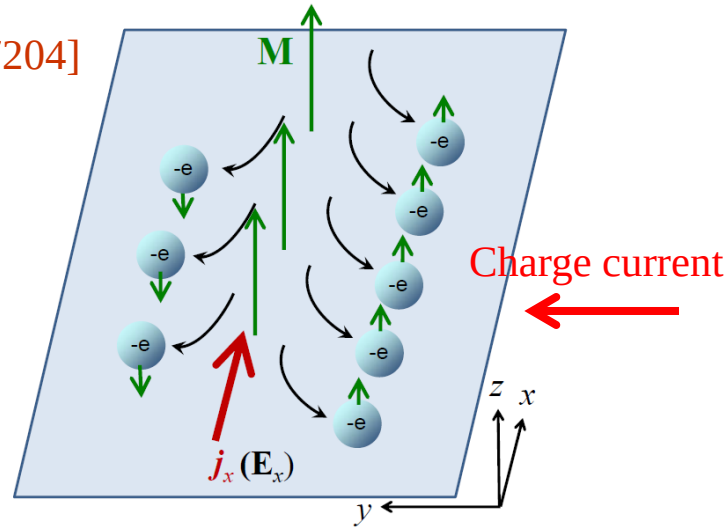

Ab initio calculations

σ_{xy} (S/cm)	theory	Exp.
bcc Fe	750[a]	1030
hcp Co	477[b]	480
fcc Ni	-1066[c]	-1100

[a][Yao, et al., PRL 92 (2004) 037204]

[b][Wang, et al., PRB 76 (2007) 195109]

[c][Fuh, Guo, PRB 84 (2011) 144427]

Integer quantum Hall effect

Hall conductance for a 2DEG in a magnetic field **B**

$$\sigma_{xy}^{H} = \frac{e^2}{\hbar}\int \frac{d^2k}{(2\pi)^2}\sum_n f_n \Omega_n^z = \frac{e^2}{\hbar}\sum_n f_n \int \frac{d^2k}{(2\pi)^2}\Omega_n^z(\mathbf{k})$$

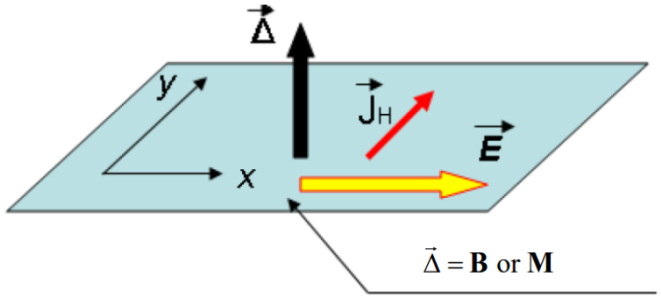

For a 2D electronic system, the BZ is a torus.

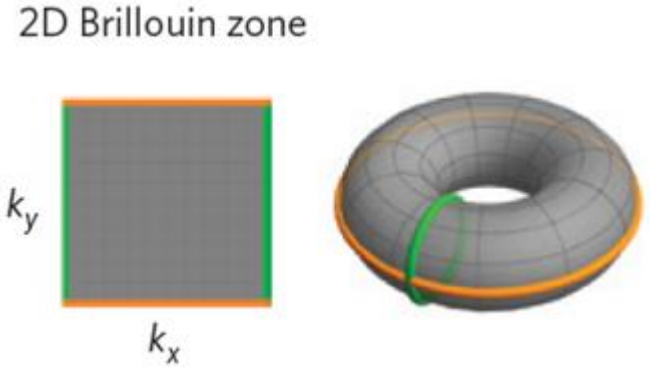

Thus, Gauss-Bonnet theorem indicates

$$\int_{\mathrm{BZ}} dk_x dk_x [\mathbf{\Omega}(k_x, k_y)]_z(\mathbf{k}) = \int_S \mathbf{\Omega}(\mathbf{k})\cdot d\mathbf{s} = 2\pi C,$$

where C is an integer (TKNN or Chern number).

This would give rise to the quantized conductance $\sigma_{xy}^{H} = \frac{2e^2}{h}C$ observed in integer quantum Hall effect

[Thouless et al., PRL49, 405 (1982)]

Spin Hall and orbital Hall effects

[Guo, Yao, Niu, PRL 94, 226601 (2005)]
[Guo et al., PRL100, 096401 (2008)]

Similarly, spin (orbital) Hall conductivity can be calculated from spin (orbital) Berry curvature,

$$\sigma_{yx}^{s/oH} = j_y^{s/o} / E_x = \frac{e^2}{\hbar}\int \frac{d^3k}{(2\pi)^3}\sum_n f(\varepsilon_{n\mathbf{k}})\Omega_n^{z,s/o}(\mathbf{k}),$$

Spin Berry curvature

$$\Omega_n^z(\mathbf{k}) = -\sum_{n'\neq n}\frac{\hbar}{e}\frac{\hbar^2\,\mathrm{Im}\left\langle n\mathbf{k}\left|\{\sigma_z, v_x\}\right|n'\mathbf{k}n\right\rangle\left\langle n'\mathbf{k}\left|v_y\right|n\mathbf{k}\right\rangle}{2(\varepsilon_{n\mathbf{k}}-\varepsilon_{n'\mathbf{k}})^2} \quad \text{(SHE)}$$

OAM Berry curvature

$$\Omega_n^z(\mathbf{k}) = -\sum_{n'\neq n}\frac{\hbar}{e}\frac{\hbar^2\,\mathrm{Im}\left\langle n\mathbf{k}\left|\{l_z, v_x\}\right|n'\mathbf{k}n\right\rangle\left\langle n'\mathbf{k}\left|v_y\right|n\mathbf{k}\right\rangle}{(\varepsilon_{n\mathbf{k}}-\varepsilon_{n'\mathbf{k}})^2} \quad \text{(OHE)}$$

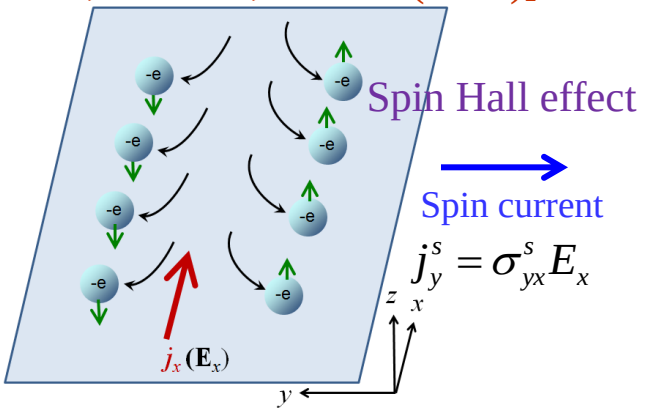

Prediction

σ_{sH} = 2100 (ħ/e)(S/cm)

Experiments:

σ_{sH} = 1700 (ħ/e)(S/cm)

[Liu et al, PRL 106, 036601 (2011)]

[Hoffmann, IEEE Trans. Mag. 49 (2013) 5172]

Predicted large SHC in Pt metal

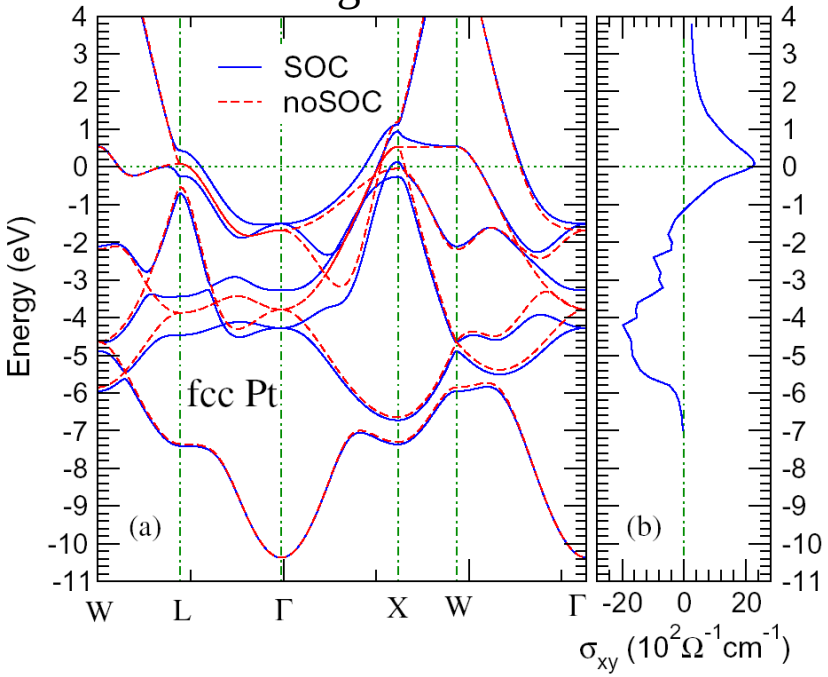

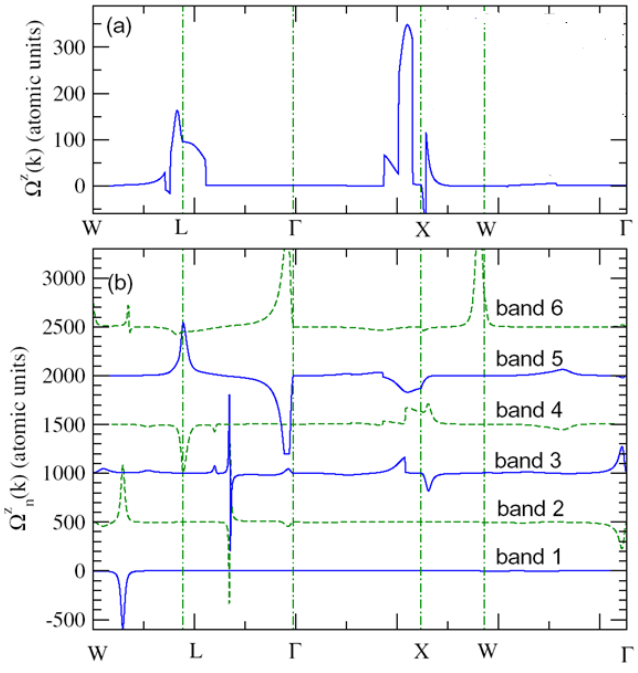

2. Nonlinear anomalous Hall effect due to Berry curvature dipole

Anomalous Hall conductivity (AHC) $\sigma_{yx} = J_y / E_x = -\frac{e^2}{\hbar}\int d^3k \sum_n f(\varepsilon_n(\mathbf{k}))\Omega_n^z(\mathbf{k})$.

For a *T*-even noncentrosymmetic solid, $\Omega_n(-\mathbf{k}) = -\Omega_n(\mathbf{k})$ and $f(\varepsilon_n(-\mathbf{k})) = f(\varepsilon_n(\mathbf{k}))$. Thus, AHC is zero.

However, breaking the occupation symmetry at **k** and –**k**, can be provided by the nonequilibrium distribution $g(\mathbf{k})$ due to an applied electric field $\boldsymbol{E}$.

In the constant relaxation time approximation, $g(\mathbf{k}) = f(\varepsilon_{\mathbf{k}}) - \frac{e}{\hbar}\tau E_c \partial_c f(\varepsilon_{\mathbf{k}})$.

This leads to the Hall current given by $J_a^{(2)H} = \sum_{b,c} \chi_{abc} E_b E_c$ where $\chi_{abc} = -\varepsilon_{abc}\frac{\tau e^3}{2\hbar^2} D_{bc}$,

with Berry curvature dipole $D_{bd} = -\int_{\mathrm{BZ}} \frac{d^3k}{(2\pi)^3}\sum_n \partial_b f(\varepsilon_{n\mathbf{k}})\Omega_n^d = \int_{\mathrm{BZ}} \frac{d^3k}{(2\pi)^3}\sum_n f(\varepsilon_{n\mathbf{k}})\partial_b \Omega_n^d$.

This is the famous NLHE in *T*-even noncentrosymmetric solid by Sodermann and Fu.

[Soldemann & Fu, PRL 115, 216806 (2015)]

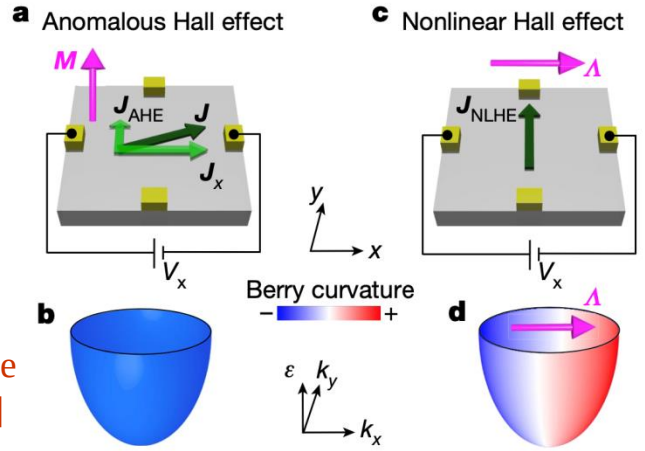

[Ma et al., Nature 565, 337 (2019)]

III. Nonlinear optical responses of solids

1. Nonlinear optical (NLO) responses of solids

[Nonlinear optics by Boyd (2003)] [Principles of NLO by Shen (2003)]

Linear and nonlinear photocurrents

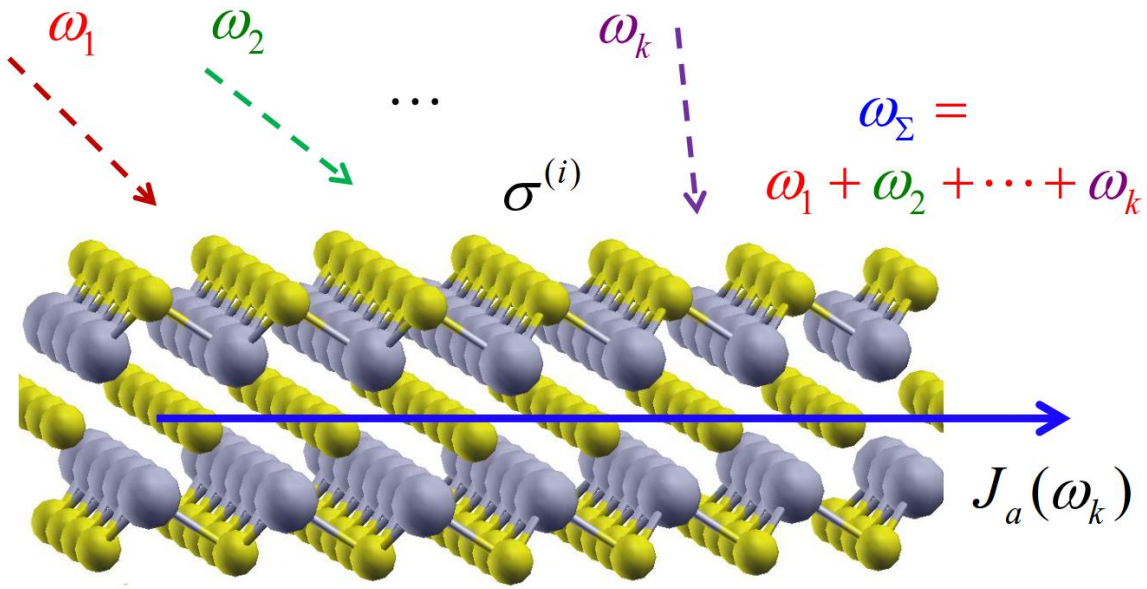

$$\mathbf{J}(\omega_\Sigma) = \sigma^{(1)}\mathbf{E}_1(\omega_1) + \sigma^{(2)}\mathbf{E}_1(\omega_1)\mathbf{E}_2(\omega_2) + \sigma^{(3)}\mathbf{E}_1(\omega_1)\mathbf{E}_2(\omega_2)\mathbf{E}_3(\omega_3) + \cdots$$

(1) Under *P*-symmetry operation,

$$\mathbf{J}(\mathbf{r}) \Rightarrow -\mathbf{J}(-\mathbf{r}); \quad \mathbf{E}(\mathbf{r}) \Rightarrow -\mathbf{E}(-\mathbf{r}).$$

Thus, even-order NLO responses can occur only in noncentrosymmetric materials.

(2) In a nonmagnetic *P*-symmetric material, the lowest NLO response of is the 3rd-order NLO effect.

2. Bulk photovoltaic effect (BPVE) [aka photogalvanic effect (PGE)]

Photovoltaic effects

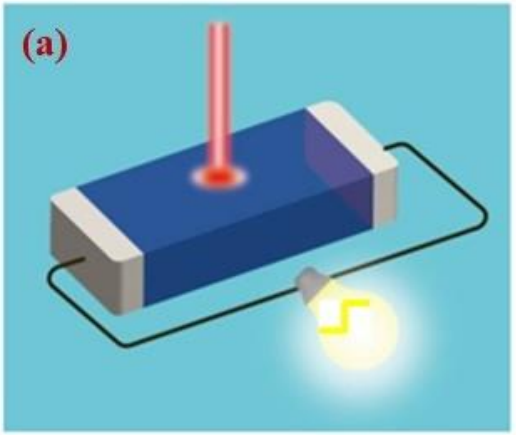

Conventional photovoltaic effect (linear response)

[Jalaja + Dutta, review,
Adv. Mater. Lett. 6 (2015) 568]

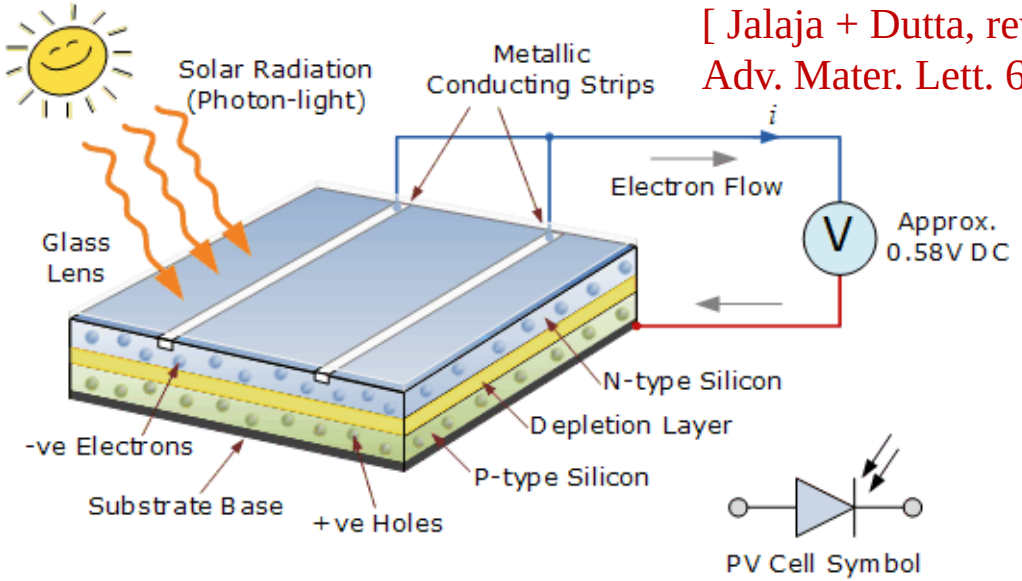

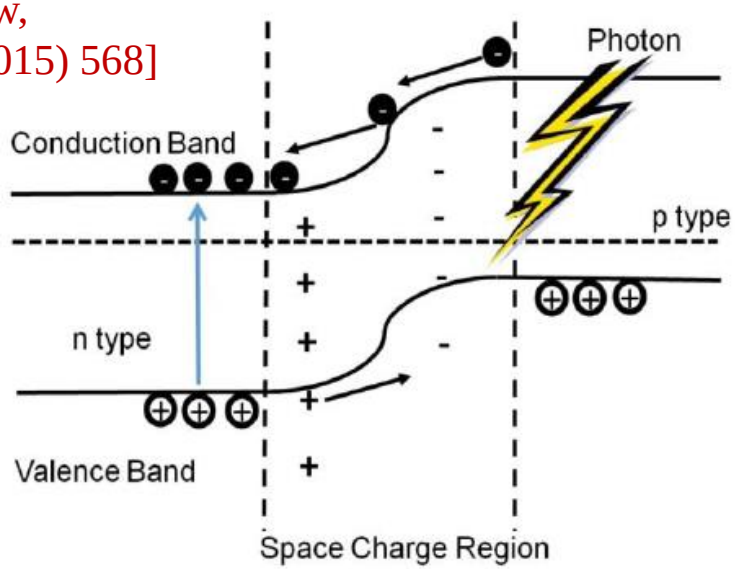

Conventional p-n junction semiconductor photovoltaic solar cells

Bulk photovoltaic effect (or BPVE) (Second-order NLO response)

dc photocurrent generation due to the (2nd-order) NLO response of *P*-assymmetric solids

$$J^{a}_{DC} = \sum_{b,c} \sigma^{abc}_{DC}(0;\omega,-\omega)E_b(\omega)E_c(-\omega) = \sum_{b,c} \sigma^{abc}_{DC}(0;\omega,-\omega)E_b(\omega)E_c(\omega)^*$$

Four types of BPVE photocurrents [Ahn, Guo & Nagaosa, PRX 10 (2020) 041041]

Light polarization

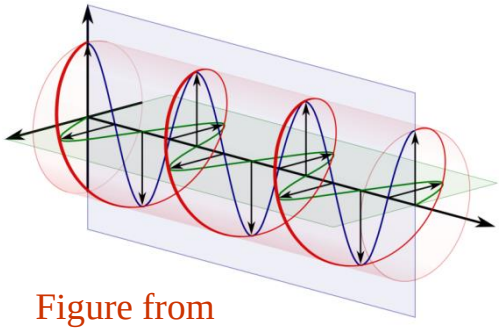

Figure from [J. Ahn]

$$J^{abc}_{DC} = \mathrm{Re}[\sigma^{abc}_{DC} E_b E_c^*]$$

$$= \frac{1}{2}\mathrm{Re}[\sigma^{abc}_{DC}](E_b E_c^* + E_b^* E_c) + \frac{1}{2}\mathrm{Im}[\sigma^{abc}_{DC}](E_b E_c^* - E_b^* E_c)$$

Non-helical — Helicity-dependent

$\mathrm{Re}[\sigma^{abc}_{DC}]$: "Linear" BPVE.

Possible for any polarization: Linear/circular/unpolarized

$\mathrm{Im}[\sigma^{abc}_{DC}]$: "Circular" BPVE.

Impossible for linear and unpolarized light

Carrier mean free time τ

Shift current $J_{sh} = \frac{dP}{dt} \propto -\int e(R_c - R_v) I_{light}$.

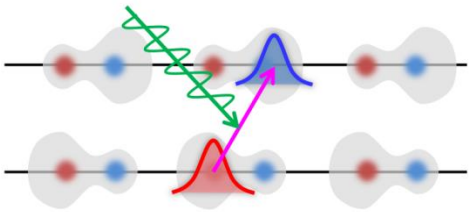

Figure from [M. Nakamura]

Injection current $J_{inj} = \tau \frac{dJ}{dt} \propto \tau \int (v_c - v_v) I_{light}$

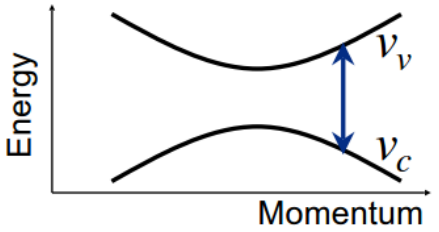

[Sipe & Shkrebtii, PRB 61 (2000) 5337]

[Young & Rappe, PRL 109 (2012) 116601]

Perturbation theory of nonlinear photocurrents

[Aversa & Sipe, PRB 52 (1995) 14636; Ahn, Guo & Nagaosa, PRX 10 (2020) 041041]

Consider a monochromatic electric field of the form

$\mathbf{E}(t) = \mathbf{E}(\omega)e^{-i\omega t} + \mathbf{E}(-\omega)e^{i\omega t}$, with $\mathbf{E}(-\omega) = \mathbf{E}^*(\omega)$,

and light-matter interaction by the electric dipole Hamiltonian $\hat{H}_{\text{int}} = e\mathbf{E}(t)\cdot\hat{\mathbf{r}}$.

Phenomenologically, the dc photocurrent density from the 2nd-order BPVE is

$$J^c = \sigma_{DC}^{c;ab}\left(0;\omega,-\omega\right)E_a(\omega)E_b(-\omega);\quad \sigma_{DC}^{c;ab} = \sigma_{sh}^{c;ab} + \sigma_{inj}^{c;ab}.$$

Within the independent particle approximation, the injection current conductivity is

$$\sigma_{inj}^{c;ab} = \tau\eta_{inj}^{c;ab}\left(0;\omega,-\omega\right) = -\frac{\tau 2\pi e^3}{\hbar^2}\int\frac{d^3k}{(2\pi)^3}\sum_{n,m} f_{nm}(v_m^c - v_n^c)r_{nm}^b r_{mn}^a \delta(\omega_{mn}-\omega).$$

Here group velocity $v_n^a = \frac{1}{\hbar}\partial_a\varepsilon_n(\mathbf{k})$. And the shift current conductivity is

$$\sigma_{sh}^{c;ab}\left(0;\omega,-\omega\right) = -\frac{i\pi e^3}{\hbar^2}\int\frac{d^3k}{(2\pi)^3}\sum_{n,m} f_{nm}\left(r_{mn}^b r_{mn;c}^a - r_{nm;c}^b r_{mn}^a\right)\delta(\omega_{mn}-\omega).$$

Here interband position matrix element $r_{mn}^a = \langle\psi_{m\mathbf{k}}\,|\,\hat{\mathbf{r}}\,|\,\psi_{n\mathbf{k}}\rangle = \langle u_{\mathbf{k}m}\,|\,i\partial_a u_{\mathbf{k}n}\rangle = A_{mn}^a$,

its generalized moment derivative $r_{mn;b}^a == \partial_b r_{mn}^a - i(A_{mm}^b - A_{nn}^b)r_{mn}^a$,

$A_{mn}^a = i\langle u_{\mathbf{k}m}\,|\,\partial_a u_{\mathbf{k}n}\rangle$ (Berry connection), $f_{mn} = f_m - f_n$ and $\hbar\omega_{mn} = \varepsilon_m(\mathbf{k}) - \varepsilon_n(\mathbf{k})$.

Complete quantum geometric meaning of BPVE

Quantum geometry of two-band Dirac Hamitonian

= geometry of generalized Bloch sphere

[Ahn, Guo & Nagaosa, PRX 10 (2020) 041041]

$$H(\mathbf{k}) = f_0 + \sum_i f_i(\mathbf{k})\sigma_i \,, (i = x, y, z);$$

$$\mathbf{f}\cdot\boldsymbol{\sigma}\left|u_\pm\right\rangle = \pm f\left|u_\pm\right\rangle, \quad f = (\sum f_i^{\,2})^{1/2}.$$

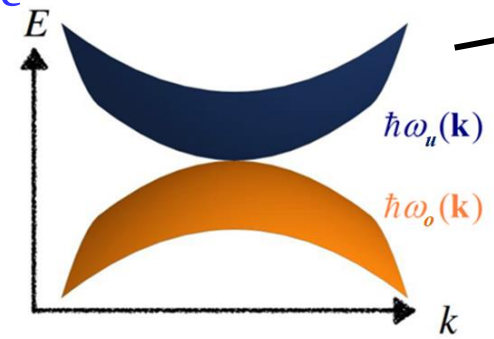

Generalized Bloch sphere

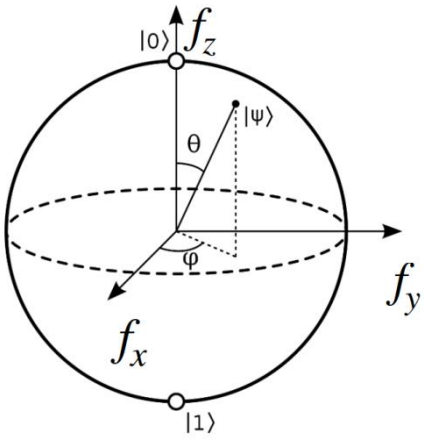

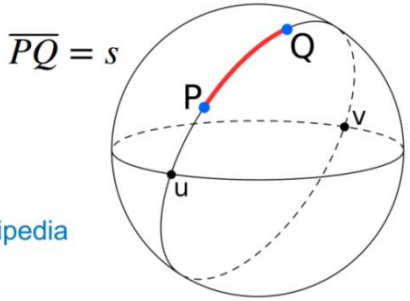

Wikipedia

Distance $ds^2 = \sum_{i,j} g_{ij} df_i df_j$

$$g_{ij} = \frac{1}{4f^2}\left(\delta_{ij} - \hat{f}_i \hat{f}_j\right)$$

metric tensor

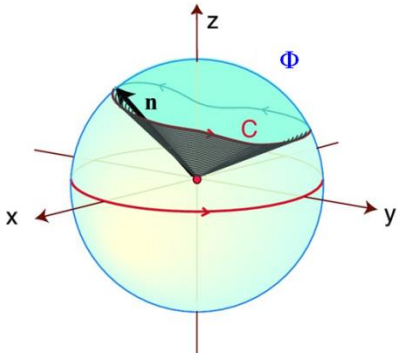

$$F_{ij} = \frac{1}{2f^2}\sum_k \varepsilon_{ijk}\hat{f}_k.$$

Symplectic form

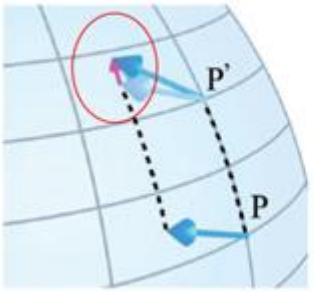

Figure: Nagaosa and Morimoto, Adv. Mater. (2017)

Parallel transport

$$\partial_j \hat{e}_k = \Gamma^i_{jk}\hat{e}_i$$

Christoffel symbols

$$\Gamma_{ijk} = \hat{e}_i \cdot \partial_j \hat{e}_k$$

$$\tilde{\Gamma}_{ijk} = \hat{n} \cdot \hat{e}_i \times \partial_j \hat{e}_k$$

$$\Gamma_{ijk} = -\frac{1}{f^2}\left(f^k g_{ij} + f^j g_{ik}\right)$$

$$= \frac{1}{2}\left(\partial_j g_{ki} + \partial_j g_{ki} - \partial_i g_{jk}\right),$$

$$\tilde{\Gamma}_{ijk} = \frac{1}{2}F_{il}(g^{-1})^{lm}\Gamma_{mjk}.$$

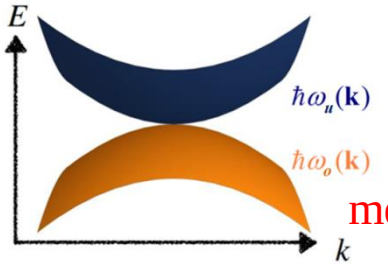

$f: BZ \rightarrow S^2$

k-space ⟵ ⟶ **Bloch sphere in f-space**

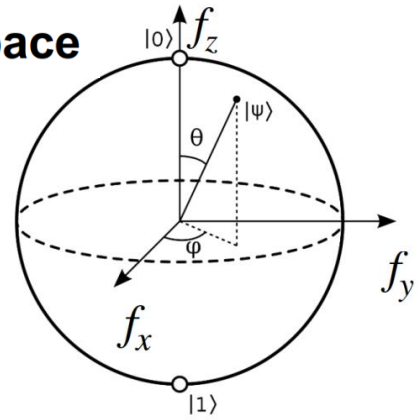

metric tensor

$$g_{ab} = \mathrm{Re}[r^a_{ou} r^b_{uo}] = \frac{\partial f_i}{\partial k_a}\frac{\partial f_j}{\partial k_b} g_{ij}$$

Berry curvature

$$\Omega_{ab} = -2\,\mathrm{Im}[r^a_{ou} r^b_{uo}] = \frac{\partial f_i}{\partial k_a}\frac{\partial f_j}{\partial k_b} F_{ij}$$

Christoffel sysmbol of 1st kind

$$\Gamma_{bca} = \frac{1}{2}(\partial_c g_{ba} + \partial_a g_{bc} - \partial_b g_{ca})$$

symplectic Christoffel sysmbol

$$\tilde{\Gamma}_{bca} = \frac{1}{2}\Omega_{bd}(g^{-1})^{de}\Gamma_{eca}$$

Hermitian connection

$$C_{bca} = r^a_{ou} r^b_{uo;c} = \Gamma_{bca} - i\tilde{\Gamma}_{bca}$$

Here o = occupied, u = unoccupied.

metric tensor g_{ij}

: measure distance
Rank-2 sym tensor

symplectic form F_{ij}

: measure area
Rank-2 antisym tensor

Christoffel sysmbol of 1st kind

$$\Gamma_{ijk} = \frac{1}{2}(\partial_j g_{ki} + \partial_k g_{ij} - \partial_i g_{jk})$$

symplectic Christoffel sysmbol

$$\tilde{\Gamma}_{ijk} = \frac{1}{2}F_{il}(g^{-1})^{lm}\Gamma_{mjk}$$

Hermitian connection

$$C_{ijk} = \Gamma_{ijk} - i\tilde{\Gamma}_{ijk}$$

$$\sigma^{c;ab}_{inj}(0;\omega,-\omega) = -\frac{\tau 2\pi e^3}{\hbar^2}\int \frac{d^3k}{(2\pi)^3}(v^c_u - v^c_o)Q_{ba}\delta(\omega_{uo}-\omega),\ Q_{ba} = g_{ba} - \frac{i}{2}\Omega_{ba}.$$

$$\sigma^{c;ab}_{sh}(0;\omega,-\omega) = -\frac{i\pi e^3}{\hbar^2}\int \frac{d^3k}{(2\pi)^3}(C_{bca} - C_{acb})\delta(\omega_{uo}-\omega).$$

Thus, the injection and shift current conductivities can be written in quantum geometric quantities.

$$\sigma_{inj,L}^{c;ab} = -\frac{\tau 2\pi e^3}{\hbar^2}\int \frac{d^2k}{(2\pi)^3}(v_u^c - v_o^c)g_{ba}\delta(\omega_{uo}-\omega),$$

$$\sigma_{inj,C}^{c;ab} = \frac{\tau\pi e^3}{\hbar^2}\int \frac{d^2k}{(2\pi)^3}(v_u^c - v_o^c)\Omega_{ba}\delta(\omega_{uo}-\omega),\ Q_{ba} = g_{ba} - \frac{i}{2}\Omega_{ba}.$$

$$\sigma_{sh,L}^{c;ab} = -\frac{\pi e^3}{\hbar^2}\int \frac{d^3k}{(2\pi)^3}(\tilde{\Gamma}_{bca} + \tilde{\Gamma}_{acb})\delta(\omega_{uo}-\omega),$$

$$\sigma_{sh,C}^{c;ab} = -\frac{\pi e^3}{\hbar^2}\int \frac{d^3k}{(2\pi)^3}(\Gamma_{bca} - \Gamma_{acb})\delta(\omega_{uo}-\omega).$$

	Linear injection	Circular injection	Linear shift	Circular shift
T-symmetric	✗	✓	✓	✗
PT-symmetric	✓	✗	✗	✓
Broken *T*	✓	✓	✓	✓
Geometric quantities	Quantum metric (g_{ab})	Berry curvature (Ω_{ab})	Symplectic Christoffel symbols $(\tilde{\Gamma}_{acb})$	Christoffel symbols of first kind (Γ_{acb})
	Quantum metric tensor $Q_{ab} = g_{ab} - i\Omega_{ab}/2$		Quantum geometric connection $C_{acb} = \Gamma_{acb} - i\tilde{\Gamma}_{acb}$	
Divergence	$O(\tau\omega^{d-3})$		$O(\omega^{d-4})$	

Quantization of circular injection current in chiral Weyl semimetal

Note: $(v_u^c - v_o^c)\delta(\omega_{uo} - \omega) = \frac{1}{\hbar}\partial_c(\varepsilon_u(\mathbf{k}) - \varepsilon_o(\mathbf{k}))\delta(\omega_{uo} - \omega)$

$= (\partial_c \omega_{uo})\delta(\omega_{uo} - \omega) = \partial_c \Theta(\omega_{uo} - \omega).$

$$\sigma_{inj,C}^{c;ab} = \frac{\tau\pi e^3}{\hbar^2}\int_{BZ}\frac{d^3k}{(2\pi)^3}(v_u^c - v_o^c)\Omega_{ba}\delta(\omega_{uo} - \omega)$$

$$= \frac{\tau\pi e^3}{\hbar^2}\int_{BZ}\frac{d^3k}{(2\pi)^3}[\partial_c\Theta(\omega_{uo} - \omega)]\Omega_{ba} = \frac{\tau\pi e^3}{\hbar^2}\int_{\omega_{uo}=\omega}\frac{d^2k}{(2\pi)^3}(\hat{n}\cdot\hat{c})\Omega_{ba}.$$

Here $\hat{n}$ is the surface normal vector, $\hat{c}$ is the unit vector of Ω_{ba}.

[de Juan et al., NC 8 (2017) 15995]

For a single Weyl cone,

$$\frac{1}{2\pi}\int_{\omega_{UO}=\omega}\frac{d^2k}{(2\pi)^3}(\hat{n}\cdot\hat{c})\Omega_{ba} = C,$$

C is the chiral charge of the Weyl node.

In a chiral Weyl semimetal, the energy levels of the Weyl nodes may be different, and thus quantized circular PVE may occur,

$$J_{\text{inj}} \propto \tau C_{\text{Chern}} \times I_{\text{light}}$$

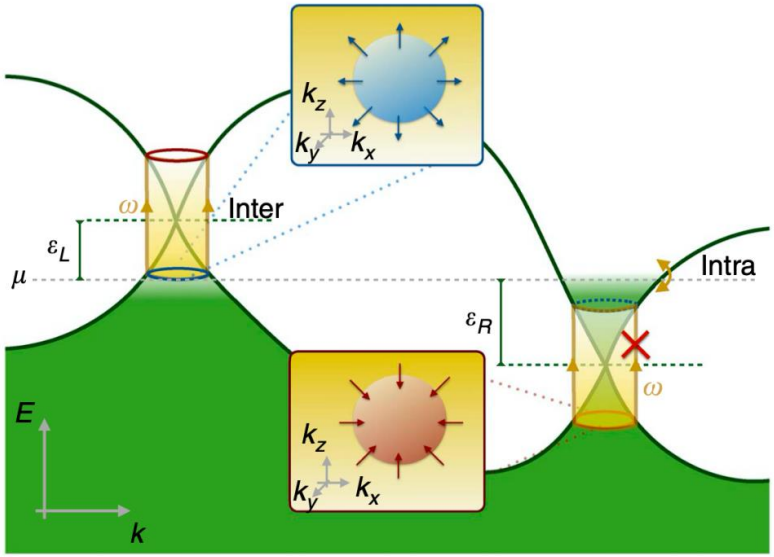

Large BPVE conductivities due to the divergent behavior of the geometric quantities near the topological points in topological semimetals

Let us consider ferromagnetic noncentrosymmetric PrGeAl

[Tsuzuki et al., JPSJ 37 (1974) 1242]

Physical properties

DOS(E_F) = 0.133 states/eV/f.u.

$m_s^{Pr} = 1.89\mu_B$,
$m_o^{Pr} = -3.83\mu_B$,
$m_s^{tot} = 1.91\mu_B$

$m_s^{Pr} = 1.89\mu_B$ (exp.)

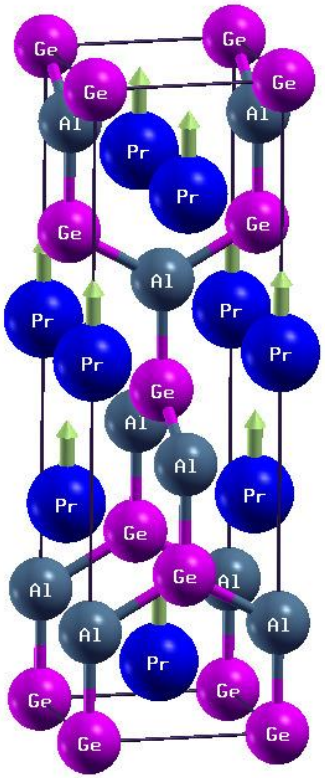

Electronic band structure

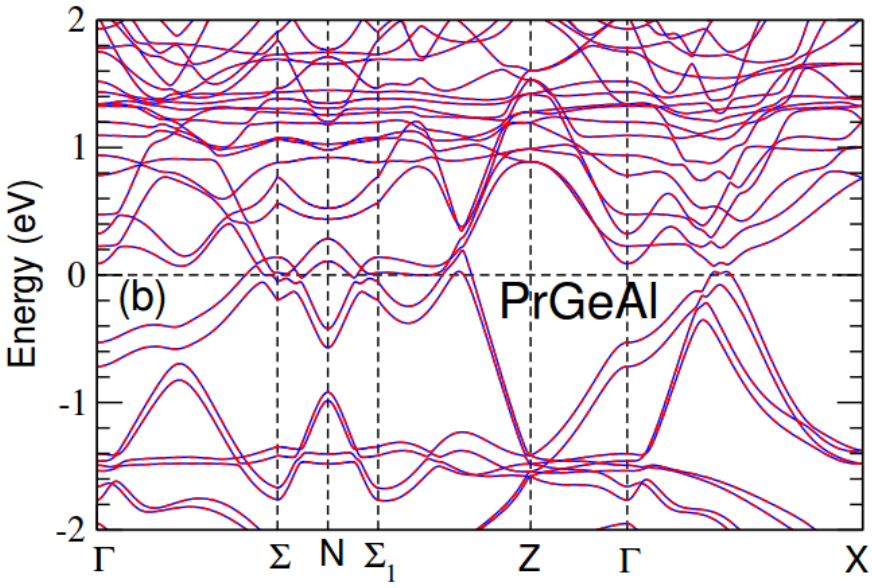

[Ahn, Guo & Nagaosa, PRX 10 (2020) 041041]

Band dispersions near the Weyl nodes

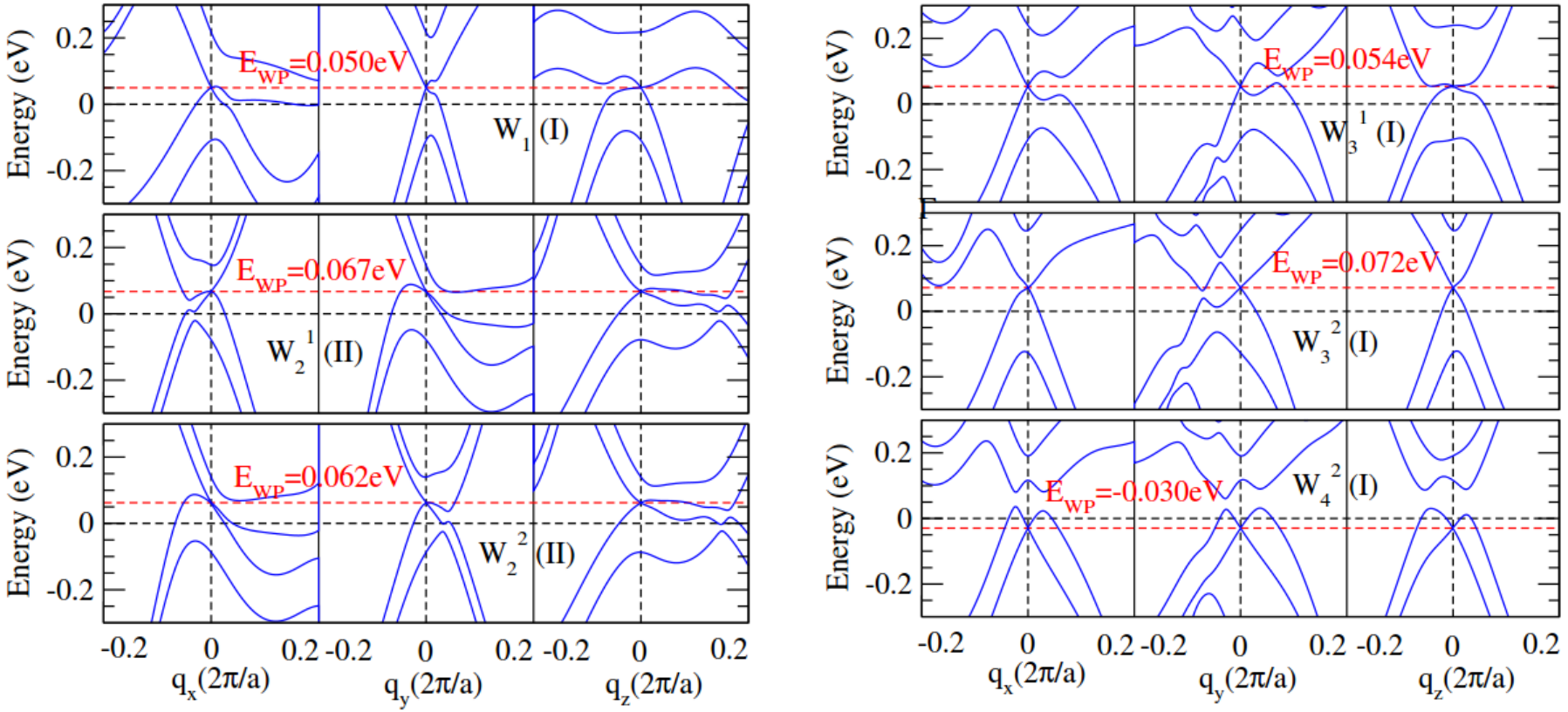

Weyl node	$K_x(2\pi/a)$	$K_x(2\pi/a)$	$K_x(2\pi/a)$	E (meV)	Type
W_1	0.4903	-0.0084	0.0269	50.04	I
W_2^1	0.0150	0.2550	0.2170	67.41	II
W_2^2	0.2570	-0.0160	0.2170	62.12	II
W_3^1	0.1600	0.2040	-0.0030	53.88	I
W_3^2	0.1680	0.2690	-0.0042	71.93	I
W_4^2	0.175	0.2190	0.0125	-29.55	I

[Ahn, Guo & Nagaosa, PRX 10 (2020) 041041]

Calculated photoconductivities and geometric quantities

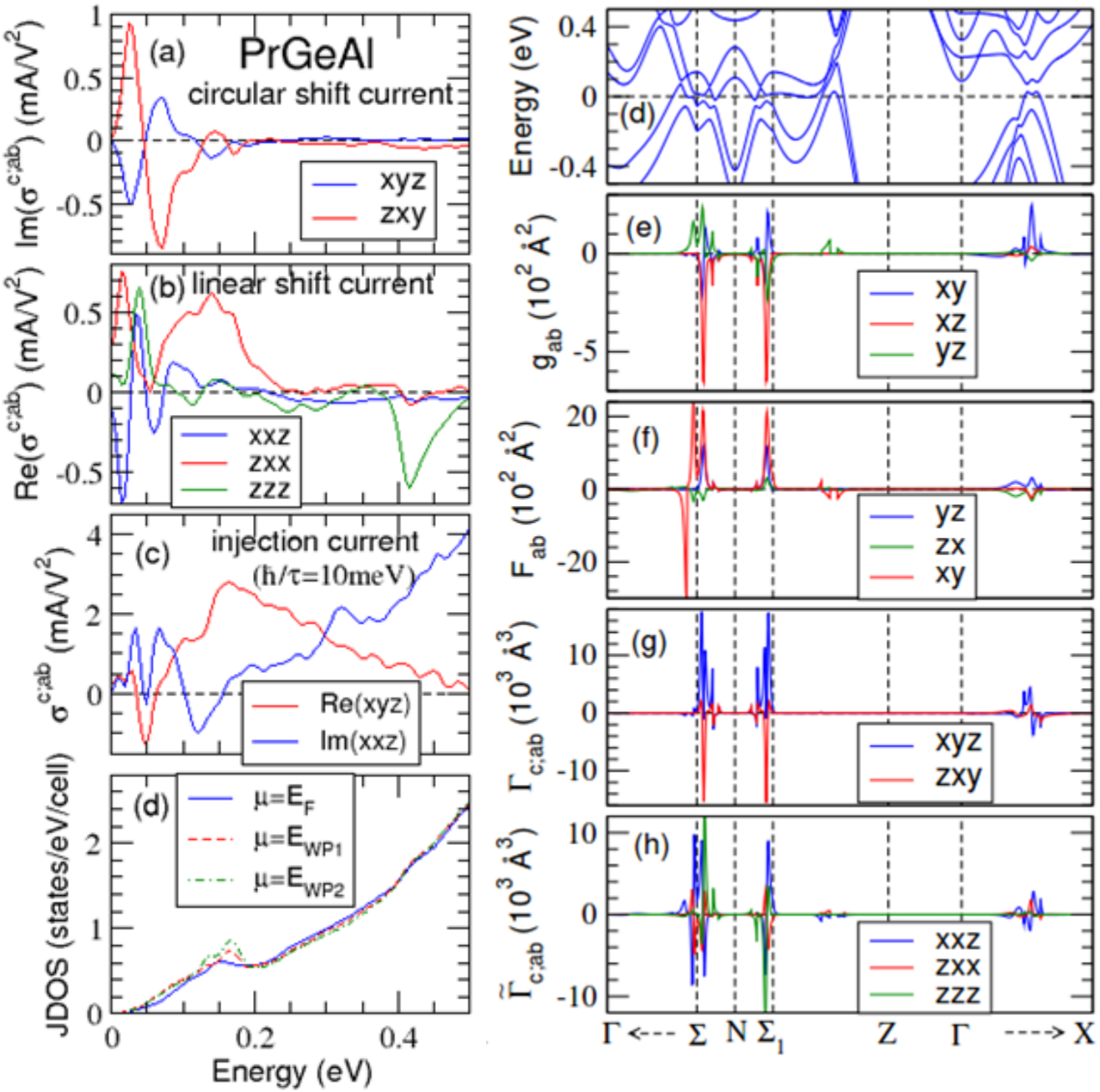

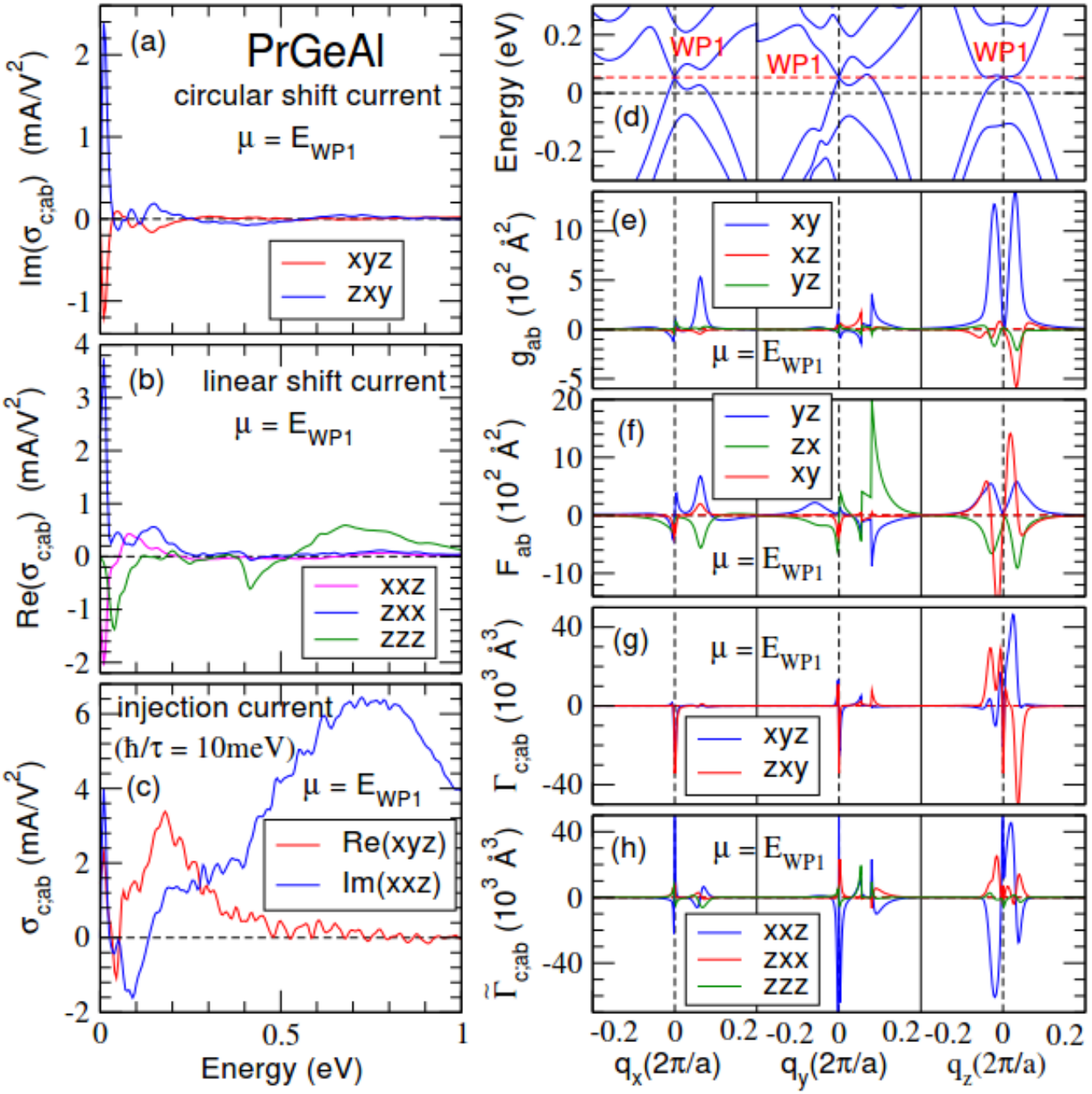
PrGeAl
(a)
circular shift current
μ = E_WP1
Im(σ_c;ab) (mA/V²)
xyz
zxy
(b)
linear shift current
μ = E_WP1
Re(σ_c;ab) (mA/V²)
xxz
zxx
zzz
injection current
(ħ/τ = 10meV)
(c)
μ = E_WP1
σ_c;ab (mA/V²)
Re(xyz)
Im(xxz)
Energy (eV)
WP1
WP1
WP1
Energy (eV)
(d)
(e)
g_ab (10² Å²)
xy
xz
yz
μ = E_WP1
(f)
F_ab (10² Å²)
yz
zx
xy
μ = E_WP1
(g)
Γ_c;ab (10³ Å³)
μ = E_WP1
xyz
zxy
(h)
Γ̃_c;ab (10³ Å³)
μ = E_WP1
xxz
zxx
zzz
q_x(2π/a)
q_y(2π/a)
q_z(2π/a)

3. Riemannian geometry of nonlinear optical responses

[Ahn, Guo, Nagaosa & Vishwanath, Nat. Phys. 18 (2022) 290]

Interaction between electron and light: electric dipole Hamiltonian

$$\hat{H}_{\text{int}} = -\hat{\mathbf{p}}\cdot\mathbf{E}(\omega) = e\mathbf{E}(\omega)\cdot\hat{\mathbf{r}} \ .$$

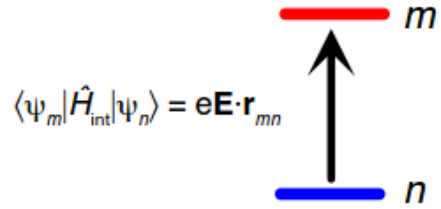

$$j^a(\omega) = \sum_k \sum_{n,m} \sigma^{a;a_1,\cdots,a_k}(\omega;\omega_1,\cdots,\omega_k) E^{a_1}(\omega_1)\cdots E^{a_k}(\omega_k).$$

Nonlinear optical conductivity: Function of

$$\mathbf{r}_{mn} = \langle \psi_{m\mathbf{k}} | \hat{\mathbf{r}} | \psi_{n\mathbf{k}} \rangle = \langle u_{m\mathbf{k}} | i\partial_{\mathbf{k}} | u_{n\mathbf{k}} \rangle$$

$\varepsilon_m(\mathbf{k}) - \varepsilon_n(\mathbf{k})$ Band structure

Interband position matrix element ($\mathbf{r}_{mn}$) contains all information on quantum geometry.

In differential geometry, tangent basis vector associated with k_i is written as ∂_{k_i}

Position operator $\hat{\mathbf{r}} \sim i\partial_{\mathbf{k}}$ is a tangent vector on some manifold.

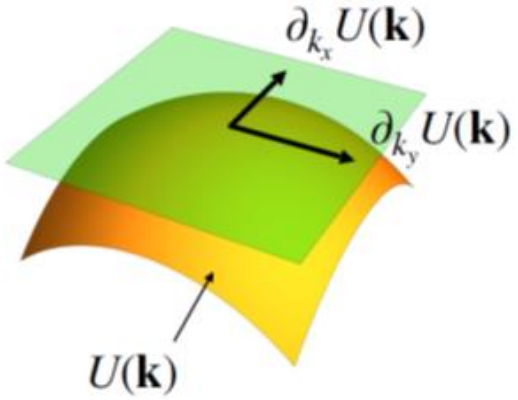

Observation: $\mathbf{r}_{mn}$ = tangent vector on manifold of cell-periodic Bloch states.

Manifold of the cell-periodic Bloch states (M)

Manifold of cell-periodic Bloch function $M = U(N)/U(1)^N$

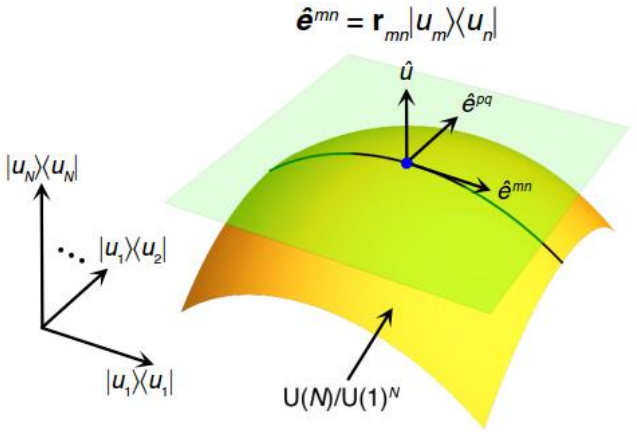

N^2-dim space of $N\times N$ matrices

[Ahn, Guo, Nagaosa & Vishwanath, Nat. Phys. 18 (2022) 290]

Transition between a pair m and n: 1-dim tangent subspace of M.

Constructing Riemannian geometry space by defining inner product and (Hermitian) metric

Natural inner product of matrices:

Hilbert-Schmidt inner product

$$(A, B) = \mathrm{Tr}(A^\dagger, B)$$

Example

$$A = \begin{pmatrix} a_{11} & a_{12} \\ a_{21} & a_{22} \end{pmatrix}, B = \begin{pmatrix} b_{11} & b_{12} \\ b_{21} & b_{22} \end{pmatrix}$$

$(A, B) = a_{11}^* b_{11} + a_{12}^* b_{12} + a_{21}^* b_{21} + a_{22}^* b_{22}$ Euclidean inner product in complex 4D

Hermitian metric (aka, quantum geometric tensor)

$$Q_{ba}^{nm} = (\hat{e}_b^{nm}, \hat{e}_a^{nm}) = r_{nm}^b r_{mn}^a.$$

$$\hat{e}_a^{nm} = r_{mn}^a \left|u_m\right\rangle\left\langle u_n\right| \text{ and } (r_{mn}^a)^* = r_{nm}^a.$$

[Ahn, Guo, Nagaosa & Vishwanath, Nat. Phys. 18 (2022) 290]

Constructing connection (parallel transport)

$$\partial_c \hat{e}_a^{nm} = \sum_b C_{ca}^b \hat{e}_b^{nm} + \Gamma_{ca}^b \hat{e}_a^{pq} + h_{ca}^b \hat{u}_b .$$

Covariant derivative

$$\nabla_c \hat{e}_a^{nm} = \sum_b C_{ca}^b \hat{e}_b^{nm} .$$

Hermitian connection

$$C_{bca}^{nm} = (\hat{e}_b^{nm}, \nabla_c \hat{e}_a^{mn}) = r_{nm}^b r_{mn,c}^a .$$

This construction clarifies the geometric meaning of the "generalized derivative",

$$O_{nm,c} = [\partial_c - iA, O]_{nm} .$$

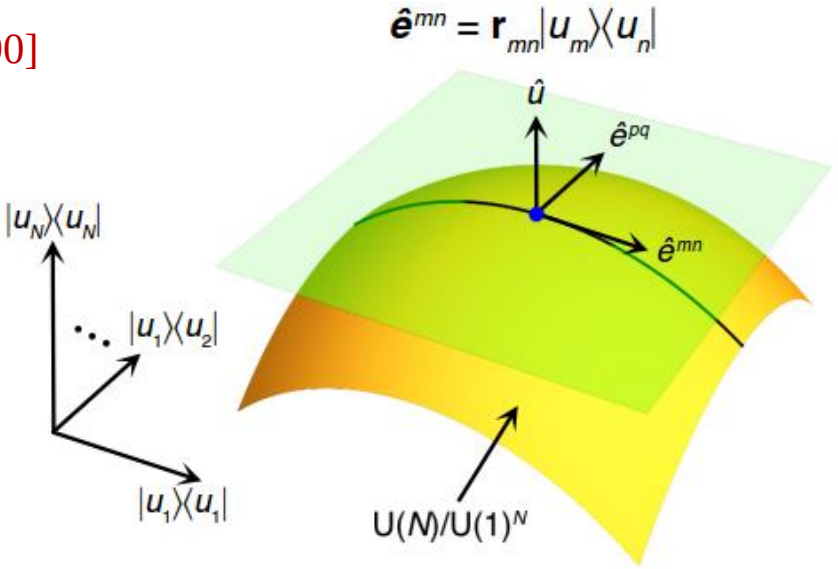

Second-order connection

$$D_{badc}^{nm} = (\hat{e}_b^{nm}, \nabla_d \nabla_c \hat{e}_a^{nm}) = r_{nm}^b r_{mn,cd}^a .$$

Hermitian curvature
(complex Riemann curvature)

$$K_{badc}^{nm} = D_{badc}^{nm} - D_{bacd}^{nm}$$
$$= (\hat{e}_b^{nm}, (\nabla_d \nabla_c - \nabla_c \nabla_d) \hat{e}_a^{nm}).$$

It is related to the Berry curvature F by

$$K_{badc}^{nm} = -i r_{nm}^b r_{mn}^a (F_{dc}^m - F_{dc}^n).$$

(Riemann curvature tensor)

Optical manifestations of Riemannian geometry of quantum states

[Ahn, Guo, Nagaosa & Vishwanath, Nat. Phys. 18 (2022) 290]

Hermitian metric (Q_{nm}^{ba}), quantum metric (g_{nm}^{ba}) and Berry curvature (F_{nm}^{ba}) in linear and second-order nonlinear optical processes

$$Q_{nm}^{ba} = r_{nm}^{b} r_{mn}^{a} = g_{nm}^{ba} - \frac{i}{2} F_{nm}^{ba}, \quad g_{nm}^{ba} = \frac{1}{2}\mathrm{Re}[r_{nm}^{b} r_{mn}^{a} + r_{nm}^{a} r_{mn}^{b}], \quad F_{nm}^{ba} = -\mathrm{Im}[r_{nm}^{b} r_{mn}^{a} - r_{nm}^{a} r_{mn}^{b}].$$

Linear optical conductivity

$$\sigma^{a;b}(\omega) = \frac{\omega e^2}{2\hbar^2 V_c} \sum_{\mathbf{k}} \sum_{n,m} f_{nm} r_{nm}^{b} r_{mn}^{a} \delta(\omega_{mn} - \omega) = \frac{\omega e^2}{2\hbar^2 V_c} \sum_{\mathbf{k}} \sum_{n,m} f_{nm} Q_{nm}^{ba} \delta(\omega_{mn} - \omega).$$

Second-order NLO injection current conductivity

$$\sigma_{inj}^{c;ab}(\omega) = -\frac{\tau 2\pi e^3}{\hbar^2 V_c} \sum_{\mathbf{k}} \sum_{n,m} f_{nm} \Delta_{mn}^{c} r_{nm}^{b} r_{mn}^{a} \delta(\omega_{mn} - \omega) = -\frac{\tau 2\pi e^3}{\hbar^2 V_c} \sum_{\mathbf{k}} \sum_{n,m} f_{nm} \Delta_{mn}^{c} Q_{nm}^{ba} \delta(\omega_{mn} - \omega),$$

$$\Delta_{mn}^{c} = v_m^c - v_n^c.$$

$$\sigma_{inj,C}^{c;ab}(\omega) = \frac{\tau\pi e^3}{\hbar^2 V_c} \sum_{\mathbf{k}} \sum_{n,m} f_{nm} \Delta_{mn}^{c} F_{nm}^{ba} \delta(\omega_{mn} - \omega), \qquad \text{(Circular injection current)}$$

$$\sigma_{inj,L}^{c;ab}(\omega) = -\frac{\tau 2\pi e^3}{\hbar^2 V_c} \sum_{\mathbf{k}} \sum_{n,m} f_{nm} \Delta_{mn}^{c} g_{nm}^{ba} \delta(\omega_{mn} - \omega), \qquad \text{(Linear injection current)}$$

Hermitian connection (C_{mn}^{bca}), Christoffel symbols (Γ_{nm}^{bca}, $\tilde{\Gamma}_{nm}^{bca}$), contorsion tensor ($K_{nm}^{bca}$) in second-order NLO processes

[Ahn, Guo, Nagaosa & Vishwanath, Nat. Phys. 18 (2022) 290]

Second-order NLO shift current conductivity

$$\sigma_{sh}^{c;ab}(\omega) = -\frac{i\pi e^3}{\hbar^2 V_c}\sum_{\mathbf{k}}\sum_{n,m} f_{nm}\delta(\omega_{mn}-\omega)(r_{nm}^{b}r_{mn,c}^{a} - r_{nm,c}^{b}r_{mn}^{a}) = -\frac{i\pi e^3}{\hbar^2 V_c}\sum_{\mathbf{k}}\sum_{n,m} f_{nm}\delta(\omega_{mn}-\omega)(C_{nm}^{bca} - (C_{nm}^{acb})^{*}).$$

[Hsu, You, Ahn & Guo, PRB 107 (2023) 155434]

Here one can find $C_{bca}^{mn} = r_{nm}^{b}r_{mn,c}^{a} = (\Gamma_{bca}^{nm} - i\tilde{\Gamma}_{bca}^{nm}) + K_{nm}^{bca}$, where $K_{nm}^{bca} = C_{bca}^{mn} - (\Gamma_{bca}^{nm} - i\tilde{\Gamma}_{bca}^{nm})$.

$$\sigma_{sh}^{c;ab}(\omega) = -\frac{i\pi e^3}{\hbar^2 V_c}\sum_{\mathbf{k}}\sum_{n,m} f_{nm}[(\Gamma_{nm}^{bca} - i\tilde{\Gamma}_{nm}^{bca}) + K_{nm}^{bca} - (\Gamma_{nm}^{acb} - i\tilde{\Gamma}_{nm}^{acb}) - K_{nm}^{acb}]\delta(\omega_{mn}-\omega).$$

Therefore,

$$\sigma_{sh,L}^{c;ab}(\omega) = -\frac{2\pi e^3}{\hbar^2 V_c}\sum_{\mathbf{k}}\sum_{n,m} f_{nm}(\tilde{\Gamma}_{nm}^{bca} + \tilde{\Gamma}_{nm}^{acb} - \mathrm{Im}[K_{nm}^{bca} + K_{nm}^{acb}])\delta(\omega_{mn}-\omega), \qquad \text{(Linear shift current)}$$

$$\sigma_{sh,C}^{c;ab}(\omega) = -\frac{i2\pi e^3}{\hbar^2 V_c}\sum_{\mathbf{k}}\sum_{n,m} f_{nm}(\Gamma_{nm}^{bca} - \Gamma_{nm}^{acb} - \mathrm{Re}[K_{nm}^{bca} - K_{nm}^{acb}])\delta(\omega_{mn}-\omega). \qquad \text{(Circular shift current)}$$

Comparison with the results of two-band Dirac Hamiltonian indicates that the contorsion tensor (K_{nm}^{bca}) terms result from multiband correction.

Third-order photovoltaic Hall effect and Riemann curvature tensor (K^{nm}_{cbad})

$$j^d_{dc} = \left[\sigma^{d;a}_{Hall} + \sigma^{d;a}_{PVH}(\omega)\right] E^a_{dc}.$$

Ordinary Hall conductivity

Third-order photovoltaic Hall conductivity

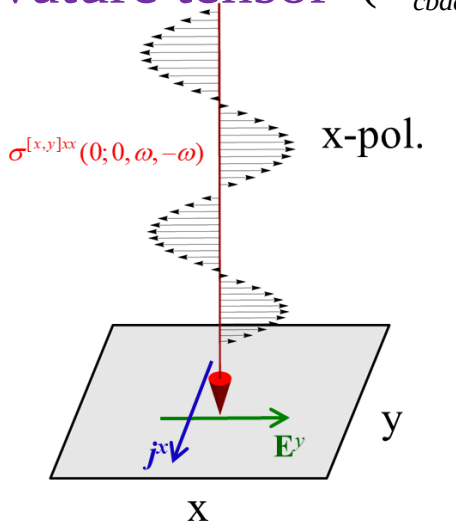

$$\sigma^{d;a}_{PVH}(\omega) = 6\sum_{a,b,c} \sigma^{d;abc}_{PVH}(0;0,\omega,-\omega) E^b(\omega) E^c(\omega).$$

$$\sigma^{c;abc}_{PVH}(0;0,\omega,-\omega) = \frac{\pi e^3}{\hbar^3 V_c}\frac{i}{6\Gamma}\sum_{\mathbf{k}} w_{\mathbf{k}} \sum_{n,m} f_{nm}\delta(\omega_{mn}-\omega)\Big\{ K^{mn}_{cbad} + \sum_e \left(C^{nm}_{edc} C^{mn|e}_{ab} - C^{nm}_{eac} C^{mn|e}_{db} \right)$$
$$+ 2\frac{\partial_d \omega_{mn}}{\omega_{mn}}\left[C^{nm}_{cba} - C^{nm}_{bca} \right] - 2\frac{\partial_d \omega_{mn}}{\omega_{mn}}\left(Q^{mn}_{ca}\frac{\partial_b \omega_{mn}}{\omega_{mn}} - Q^{nm}_{ba}\frac{\partial_c \omega_{mn}}{\omega_{mn}} \right)$$
$$+ 2\partial_d \sum_{p:p\neq m,n} \left[r^c_{nm}\left(r^b_{mp}\frac{r^a_{pn}}{\omega_{pn}} - \frac{r^a_{mp}}{\omega_{mp}} r^b_{pn} \right) + \left(r^c_{np}\frac{r^a_{pm}}{\omega_{pm}} - \frac{r^a_{np}}{\omega_{np}} r^b_{mn} \right) r^c_{pm} \right] \Big\}.$$

Table 1 | Properties of the third-order photoconductivity tensors

Response	Jerk linear	Injection linear	Injection circular	Shift linear	Shift circular
Photovoltaic Hall effect	No	Yes	Yes	Yes	Yes
T or *PT* symmetry	Yes	No	Yes	Yes	No

[Ahn, Guo, Nagaosa & Vishwanath, Nat. Phys. 18 (2022) 290]

Circular PVHE of 3D massive Dirac fermion

Two-band model $H(\mathbf{k}) = \hbar v(k_x\tau_z\sigma_x + k_y\tau_z\sigma_y + k_z\tau_z\sigma_z) + m\tau_x.$

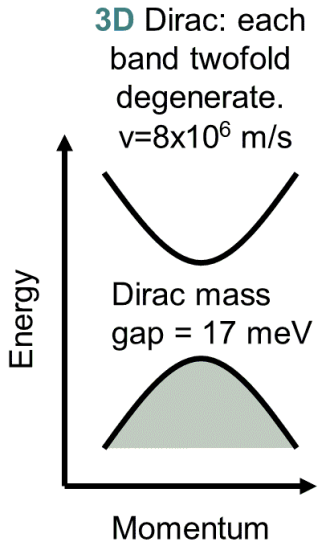

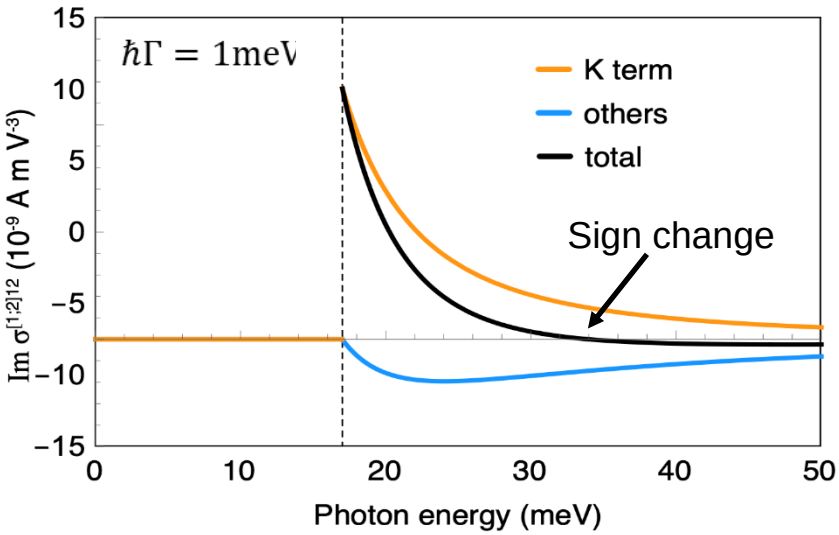

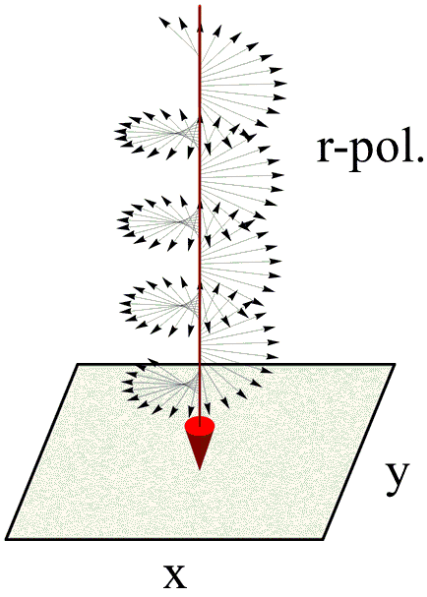

$$\sigma_{\mathrm{CPVH}} = \frac{e^4}{36\hbar^3}\frac{1}{\Gamma}\frac{1}{\omega}\left(\frac{v}{\omega}\right)\left\{1 + 2\left(\frac{2m}{\hbar\omega}\right)^{\epsilon} - 2\right|1 -$$

Riemann curvature tensor

The others

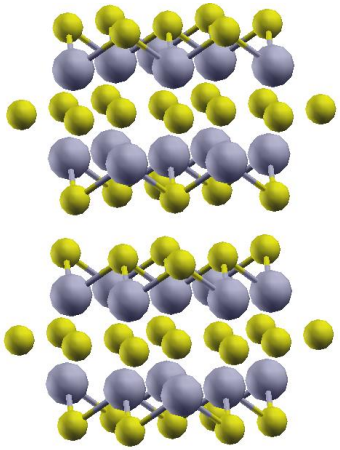

Bulk Bi_2Se_3

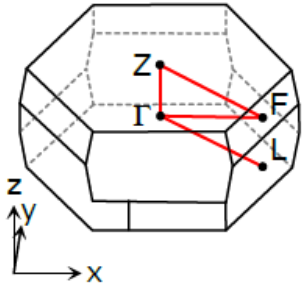

3D Z_2 TI

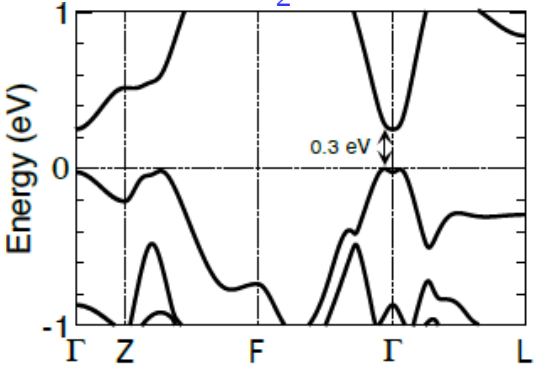

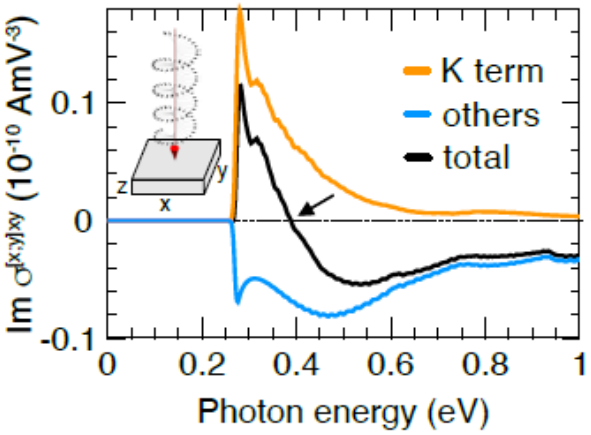

IV. Summary

1. Quantum geometry concerns the geometric structure quantum state space, e.g., quantum distance, metric and curvature. The quantum geometry approach has led to better understanding of electrical transports in solids, e.g., AHE, SHE, QHE, and also to the discovery of exotic phenomena, e.g., SHE, NLHE.

2. Two-band Dirac Hamiltonian and ab initio calculations reveal giant 2^{nd}-order nonlinear photocurrents in topological semimetals due to the divergent behavior of geometric quantities near the Dirac and Weyl nodes.

3. By identifying transition dipole moment matrix elements as tangent vectors, one can construct a Riemannian geometry for resonant optical processes, thus showing that optical responses of all orders are manifestations of the geometry of quantum state space.

Acknowledgements

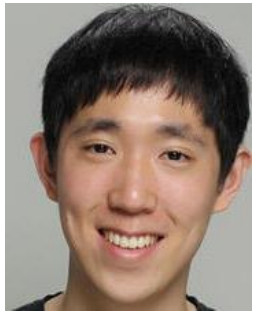

Junyeong Ahn

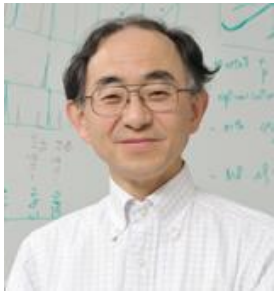

Naoto Nagaosa

Ashivin Vishwanath

Supports

NSTC 國家科學及技術委員會
National Science and Technology Council

NCTS

Thank you for your attention!